

## Preliminary study of a dispersed fringe type sensing system \*

Yong Zhang<sup>1,2</sup>, Gen-Rong Liu<sup>1,2</sup>, Yue-Fei Wang<sup>1,2</sup>, Ye-Ping Li<sup>1,2</sup>, Ya-Jun Zhang<sup>1,2</sup> and Liang Zhang<sup>1,2,3</sup>

<sup>1</sup> National Astronomical Observatories / Nanjing Institute of Astronomical Optics & Technology, Chinese Academy of Sciences, Nanjing 210042, China; [yzh@niaot.ac.cn](mailto:yzh@niaot.ac.cn)

<sup>2</sup> Key Laboratory of Astronomical Optics & Technology, Nanjing Institute of Astronomical Optics & Technology, Chinese Academy of Sciences, Nanjing 210042, China

<sup>3</sup> Graduate University of Chinese Academy of Sciences, Beijing 100049, China

Received 2009 January 16; accepted 2009 March 24

**Abstract** Telescopes with large aspherical primary mirrors collect more light and are therefore sought after by astronomers. Instead of using a single large one-piece mirror, smaller segments can be assembled into a useable telescopic primary. Because the segments must fit together to create the effect of a single mirror, segmented optics present unique challenges to the fabrication and testing that are absent in monolithic optics. A dispersed fringe sensor (DFS) using a broadband point source is an efficient method for cophasing and is also highly automated and robust. Unlike the widely adopted Shack-Hartmann Wavefront sensor and curvature wavefront sensor with edge sensors for calibration of relative pistons, DFS can estimate the piston between segments by only using the spectrum formed by the transmissive grating's dispersion, and therefore can replace the edge sensors, which are difficult to calibrate. We introduce the theory of the DFS and Dispersed Hartmann Sensor (DHS) for further utilization of the coarse phasing method of DFS. According to the theory, we bring out the preliminary system design of the cophasing experimental system based on DFS and DHS which is now established in our institute. Finally, a summary is reached.

**Key words:** instrumentation: active optics — techniques: image processing — techniques: spectroscopic — telescope: cophasing sensor

### 1 INTRODUCTION

To collect more light and increase resolution and sensitivity, researchers have expended tremendous efforts in recent years to increase the size of telescopic primary mirrors. Large primary mirrors with excellent optical system performance can give much sharper images, since the angular resolutions of the telescopes are increased. At the limit of diffraction, angular resolution is given by  $\lambda/D$ , where  $\lambda$  is the wavelength of observation and  $D$  is the diameter of the primary mirror.

The principal difficulty in the manufacture of a large telescope is the fabrication of the primary mirror. In the case of ground-based telescopes, making monolithic primary mirrors larger than 8 m is unfeasible owing to difficulties in support, transportation and manufacture of monolithic mirror blanks. In the case of large-space telescopes when the launch vehicles are not large enough, the mirror must be folded during launch. In either case, the primary mirror of a very large telescope must be constructed

---

\* Supported by the National Natural Science Foundation of China.

from smaller segments. Segmenting large primary mirrors into smaller pieces during the mirrors' manufacturing stages allows the construction of ever-larger telescopes. If the segments are manufactured and positioned perfectly, the optical performance of the mirror is identical to that of a mirror with a continuous surface, except for the light missing from the small gaps between segments.

Segmented mirrors, however, create some unique challenges for the fabrication and testing process. A segmented primary mirror requires that all segments of the primary mirror be correctly phased together to ensure that the mosaic of segments has the same optical shape as an ideal single continuous surface. The tolerance and alignment requirements for each of the segments are much tighter than those for conventional optics. Currently, there is a lack of an established method that can test a large quantity of off-axis aspherical mirror segments accurately, quickly, and economically. This paper further develops a new method of testing segmented mirrors that can potentially achieve accuracy and efficiency and be reasonably cost effective.

As we know, the LAMOST project (Su et al. 1998; Wang et al. 1996; Su & Cui 2004; Zhang 2005; Zhang 2006; Cui et al. 2004; Yuan et al. 2006; Zhang et al. 2004; Zhang & Cui 2005; Zhang 2008), which is the only large telescope in China, will soon be finished, and telescope construction plans with much larger apertures are being considered for developing Chinese astronomy. In these projects, cophasing technology is an especially important key technology, and should be developed and demonstrated before the construction of extremely large telescopes begins. Before the approval of the LAMOST project, Academician Dingqiang Su led the set up of two indoor active optics experimental systems in the Nanjing Institute of Astronomical Optics and Technology, Chinese Academy of Science (NIAOT, CAS) (Su et al. 1994; Su et al. 2000). One is for deformable mirror active optics research and the other (Fig. 1) is for segmented mirror active optics research. The success of both systems in the last century had laid an important foundation for the establishment of the LAMOST project. LAMOST begins from them.

The Dispersed Fringe Sensor (DFS) and Dispersed Hartmann Sensor (DHS) are efficient and robust methods adopted for coarse phasing of a segmented primary mirror such as the James Webb Space Telescope (JWST) during its initial deployment. Simulations, analysis and even laboratory tests have already been carried out to demonstrate the success of DFS and DHS for the JWST (Wirth 2000; Smith

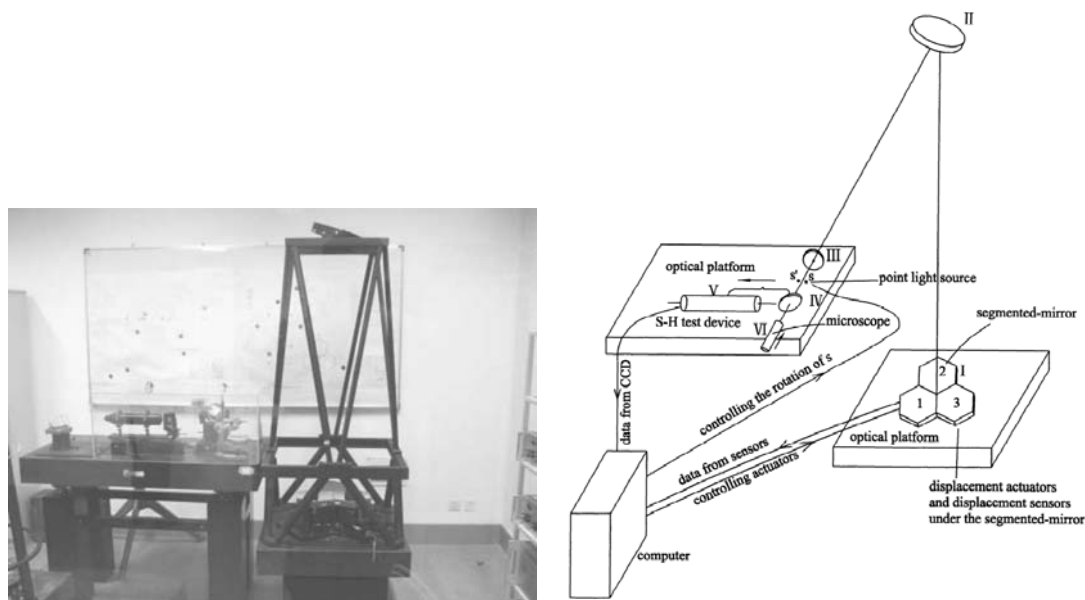


**Fig. 1** Indoor segmented active optics experiment system built in 1994 in NIAOT.

et al. 2003; Shi et al. 2002; Burns et al. 2004). It is different from the mature and widely used Shack-Hartmann wavefront sensor and curvature wavefront sensor with edge sensors for calibration of relative pistons. DFS can estimate the piston only by the spectrum formed by the transmissive grating's dispersion, and therefore can replace the edge sensors, which are difficult to calibrate. To make better use of the already existing indoor segmented mirror active optics system platform and to grasp the new cophasing technology, a project of Cophasing Segmented Active Optics Dispersed Fringe Sensing (CSAODFS) research has been approved and supported by the National Natural Science Foundation of China (NSFC) since 2008. The core of the project is to build a sensor and phase the segments in the lab segmented active optics experiment system (Fig. 2).

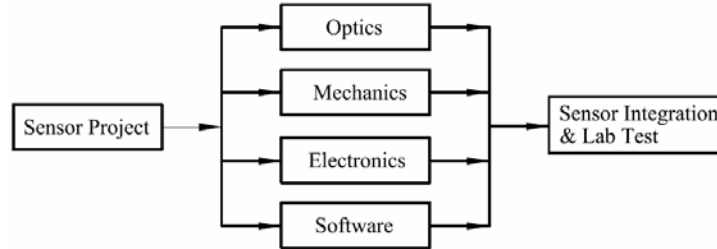


Fig. 2 Project Layout of CSAODFS system.

The main specification of the CSAODFS is for testing the pistons and cophase the segmented active optics experimental system with a cophasing precision of  $\lambda/10 \sim \lambda/15$  (mirror precision RMS,  $\lambda=650$  nm, segmented aperture =220 mm) before the end of 2010.

## 2 PRINCIPLE OF DISPERSED FRINGE SENSOR FOR SEGMENTED MIRROR PISTON DETECTION

The dispersed fringe sensor uses a transmissive grism as the dispersing element. The grism disperses the light from a broadband source according to its wavelength, forming a spectrum on the camera. The wavelength dispersion relation along the dispersion direction  $x$  is

$$\lambda(x) = \lambda_0 + \frac{\partial \lambda}{\partial x} \cdot x = \lambda_0 + C_0 \cdot x, \quad (1)$$

where  $\lambda_0$  is the central wavelength and  $C_0$  is the linear dispersion coefficient, which depends on the characteristics of the grism. Coherent addition of the wavefront errors due to the relative piston of the segmented mirrors will result in intensity modulation within the spectrum. The field intensity at any point  $E(x)$  along the dispersion is the sum of the fields  $E_1$  and  $E_2$  from the de-phased segments,

$$E(x) = E_1 e^{i[2\pi/\lambda(x)L]} + E_2 e^{i[2\pi/\lambda(x)(L+\delta L)]}. \quad (2)$$

Here  $x$  is the dispersion direction coordinate,  $\lambda(x)$  is the wavelength dispersion along the dispersion direction,  $L$  is the common optical path and  $\delta L$  is the phase difference between segments. An approximate but general derivation has shown that the intensity along the fringe has the form (3) of,

$$I(x, y) = I_0 \left[ 1 + \gamma \cdot \cos \left( 2\pi \frac{\delta L}{\lambda(x)} + \Phi(y) \right) \right], \quad (3)$$

where  $I(x, y)$  is the DFS fringe intensity along the dispersion coordinate  $x$ ,  $I_0$  is the mean intensity,  $\gamma$  is the fringe visibility which varies between 0 and 1, and  $\Phi$  is a phase constant that depends on where the DFS fringe is extracted.  $\Phi$  is zero at the fringe center ( $y=0$ ). Generally, the intensity of the central

row pixels along the dispersion is used as the main DFS signal. It is chosen because it has the highest intensity level. According to Equation (3), a typical DFS image and signal are listed below to express the DFS characteristic (Figs. 3 and 4). We can also find that the fringe modulation period is related to the piston error – a larger piston will cause more fringes.

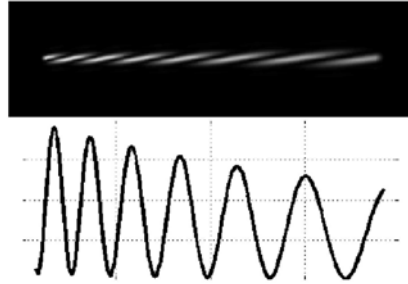


**Fig. 3** DFS image (*upper*) and DFS signal (*lower*).

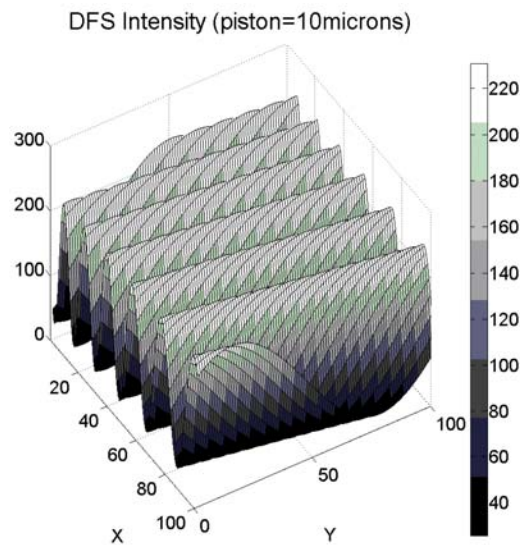


**Fig. 4** Spatial distribution of DFS intensity.

### 3 PRELIMINARY STUDY OF COPHASING SEGMENTED ACTIVE OPTICS DISPERSED FRINGE SENSOR

Equation (3) tells us that the fringe modulation period is related to piston error – a larger piston will cause more fringes, and a smaller piston will produce less fringes. In the following figure (Fig. 5), theoretical DFS fringes with pistons from 90 to 0 microns are given in a  $400 \times 400$  CCD pixel area with a visible spectrum bandwidth of 200 nm from 400 nm to 600 nm.

From Equation (3), we can find that the fringe visibility has a big impact on the test of the DFS fringes, which especially affects the accuracy of the test. Here, we can simulate the effects with different visibility on different relative pistons. However, no great influences have ever been found (Figs. 6 and 7).

When the relative piston is less than one wavelength, the frequency of the fringe decreases and it is not enough to repeat the test. Because the lower limit of the detection range is larger than one

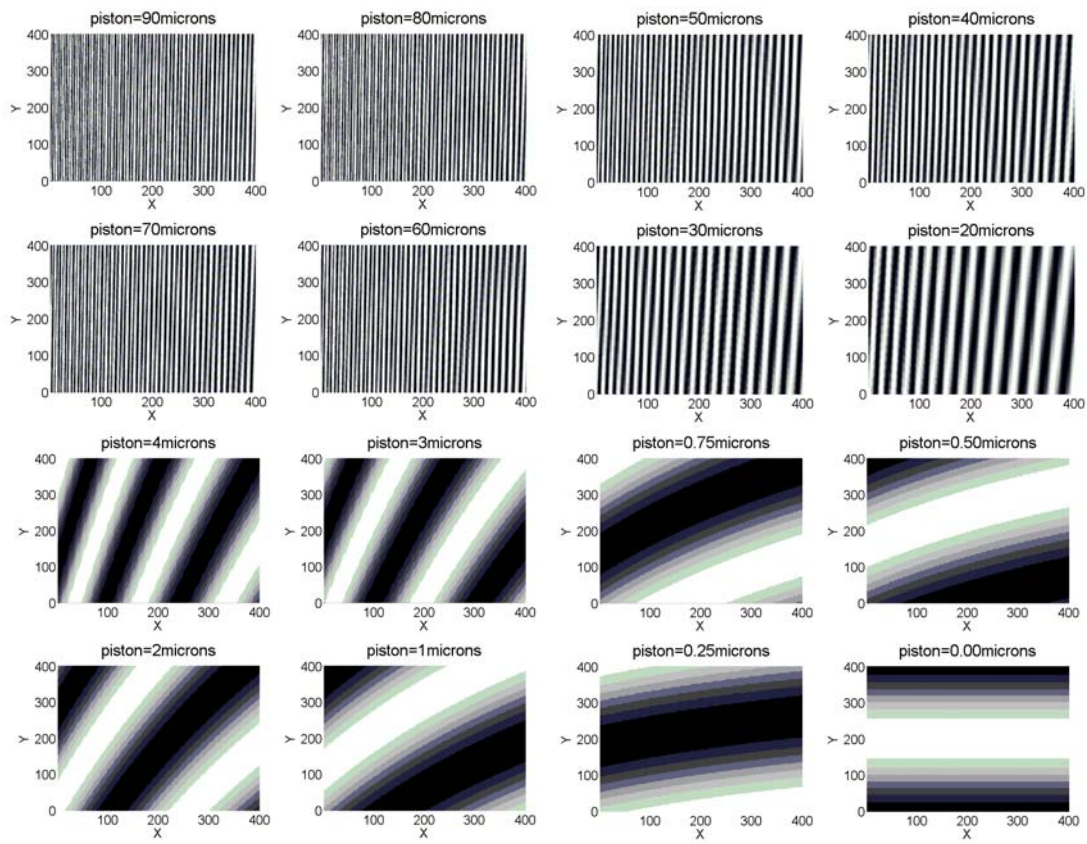


**Fig. 5** Fringes with different pistons from 90 to zero microns.

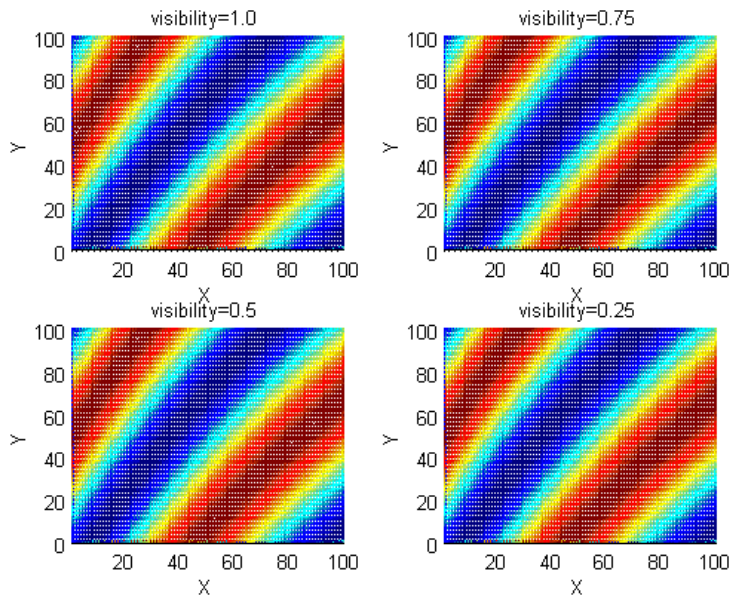


**Fig. 6** DFS fringes with different visibility while the relative piston is at 2 microns.

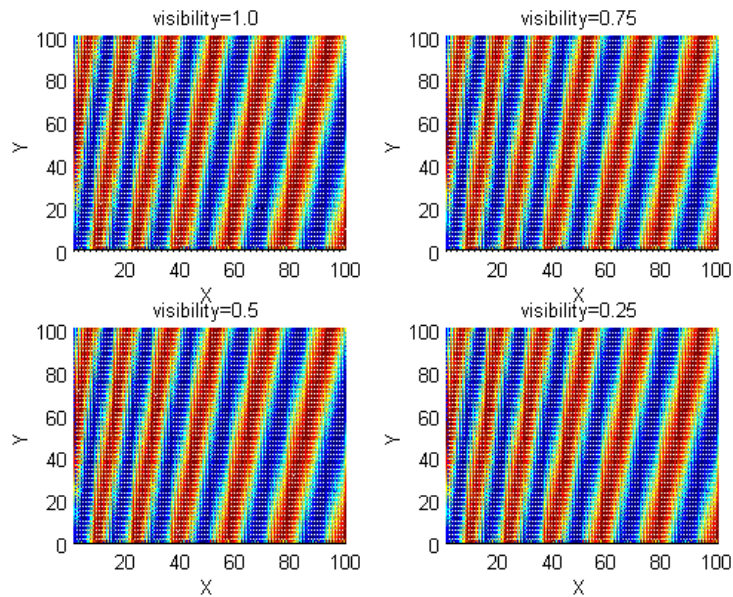


**Fig. 7** DFS fringes with different visibility while the relative piston is at 10 microns.

wavelength, DFS is only used as a coarse cophasing method for the JWST. Therefore, for our cophasing goal, we have to expand the lower limit of detection to be less than one wavelength, even to a small fraction of the wavelength. This is currently the most pressing issue in our project.

There are two ways to expand the detection area of DFS to a fraction of a wavelength. The first one is to use a known size of wave plate, which introduces an optical path difference  $L$ , e.g. several wavelengths  $L = n\lambda$ , into the light path and the small fraction of wavelength  $\delta L$ , which is less than  $\lambda$ , can be solved from the large piston  $L + \delta L$  indirectly. By using this way of moving the measuring rule, finally the aim of spreading the range of DFS can be realized. Certainly, it is important to make sure that the detection error of  $L + \delta L$  and further  $\delta L$  can reach the specification of our project, which aims at less than one-tenth of a wavelength. According to the principle of DFS, it just needs to spread the spectrum from a wide-band light source onto a large enough CCD target area, which will influence the automation while phasing a quantity of segments.

The second is the DHS, whose design is based on a dispersed fringe sensor and a traditional Hartmann sensor. Compared to a DFS grism, DHS has, in addition to the grism, an array of cross-dispersing displacement prisms which separate the dispersed fringes away from each other and also a Hartmann lenslet array to force the piston detection to be in the range of less than one wavelength without the ambiguity of a half-wave. Like DFS, if a Hartmann spot is dispersed parallel to the edge of the phase step, we may observe the shape of the blurred spot formed by a Hartmann lenslet combined with a dispersive element at many wavelengths. At each line perpendicular to the dispersion, the light distribution will be characteristic of the blurred spot formed by a Hartmann sensor at one particular wavelength (Fig. 8). That is the basic principle of DHS. A DHS can simultaneously form dispersed fringes from many inter-segment edges in one image, which can be realized much more robustly and automatically compared to the first method above.

The CSAODFS has many elements such as the grism, lenslet array, and CCD camera designed to be compatible with the current existing segmented mirror active optics three-segment experimental system (Figs. 1 and 9). The experimental test of our system will be done in the auto-collimation test light path in Figure 3.

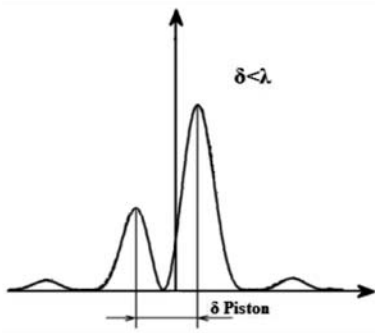


Fig. 8 DHS fringe profile perpendicular to the dispersion direction.

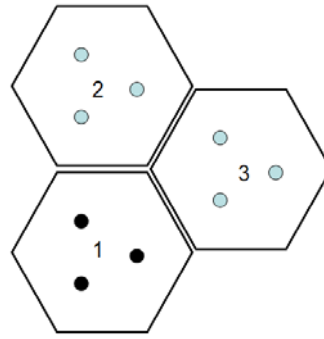


Fig. 9 Distribution of actuators at the back of the segmented mirror experiment system (Segment 1 is fixed).

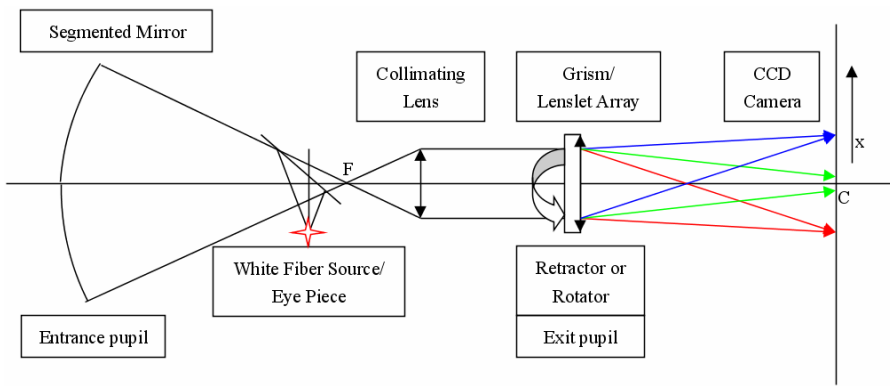


Fig. 10 System test layout of CSAODFS.

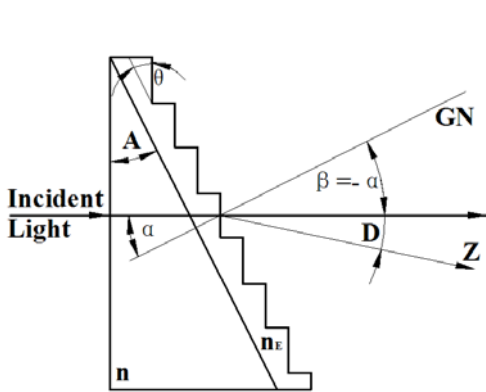


Fig. 11 Grism design principle.

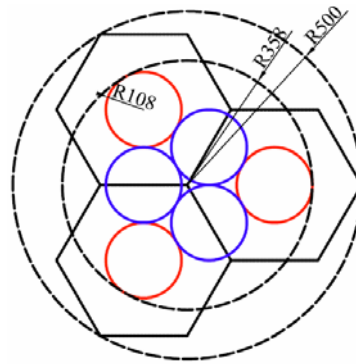


Fig. 12 Lenslet array corresponding to the entrance pupil.

At present in our project, the optical system of the DHS sensor has been designed and assembled and the key optical components, such as the grism (Fig. 11) and lenslet array (Fig. 12), have been put into manufacture. A much more careful optical design with the exact type and parameters of optical components will be carried out at the beginning of this year, followed by the electromechanical design.

The grism can be designed by choosing suitable parameters such as apex angle or groove angle  $A$ , grooves per mm and blaze wavelength which were first ordered from a commercial product catalog. However, in China, this is difficult to manufacture, so we resorted to Richardson Grating in the US for a customization of the grism with both prism and grating glued to each other, which cost us a lot of time.

There are two types of sub-apertures, including a normal aperture in the center of the segment for tilt and a smaller aperture for cofocusing control. After minimizing the tilt error, DHS is used to measure piston differences, and then do phasing. With DHS 2D image distribution section data along the dispersion direction and across the dispersion direction, piston errors among segments can be precisely measured and resolved, and then the segment phasing could be realized.

#### 4 SUMMARY

As is well known, DFS is adopted by JWST's coarse phasing, which can lower the relative piston to about several microns. It is a big problem to extend the minimum limit to one tenth of a wavelength whose scale is about several tens of nanometers. There is a DFS type sensor under construction which will be used to test and phase the lab segmented mirror experiment system. Two methods have been considered together to build the sensor. They are both feasible. The first is to use a known wave plate, which will induce a known piston  $L$  which is in the range of the DFS test system. Now, the piston  $L + \delta L$  can be measured accurately, as can the indirect small piston  $\delta L$ . The only shortcoming of this method is that it needs a large CCD and cannot be automated. The second is to use a DHS, which can eliminate the ambiguity of the half-wave and estimate the piston to less than one wavelength. DHS is a much more feasible and even more promising way to phase the segmented mirror, especially for a space telescope without atmospheric turbulence. A phasing sensor based on this DHS concept has been carried out and the preliminary design with some simulations is also presented.

**Acknowledgements** This work is supported by the National Natural Science Foundation of China (Grant No. 10703008).

#### References

- Burns, L. A., Basinger, S. A., et al. 2004, Proc. SPIE, 5487, 918  
 Cui, X. Q., Su, D. Q., Li, G. P., et al. 2004, Proc. SPIE, 5489, 974  
 Smith, E. H., Vasudevan, G., et al. 2003, Proc. SPIE, 4850, 469  
 Shi, F., Redding, D. C., Lowman, A. E., et al. 2002, Proc. SPIE, 4850, 318  
 Su, D. Q., Jiang, S. T., & Zou, W. Y., et al. 1994, Proc. SPIE, 2199, 609  
 Su, D. Q., Cui, X. Q., Wang, Y. N., & Yao, Z. Q. 1998, Proc. SPIE, 3352, 76  
 Su, D. Q., Zou, W. Y., & Zhang, Z. C., et al. 2000, Proc. SPIE, 4003, 417  
 Su, D. Q., & Cui, X. Q. 2004, ChJAA (Chin. J. Astron. Astrophys.), 4, 1  
 Wang, S. G., Su, D. Q., et al. 1996, Applied Optics, 35, 5155  
 Wirth, A. 2000, Proc. SPIE, 4003, 250  
 Yuan, X. Y., Cui, X. Q., Liu, G. R., Zhang, Y., & Qi, Y. J. 2006, Proc. SPIE, 6272, 62723O  
 Zhang, Y., Yang, D. H., & Cui, X. Q. 2004, Applied Optics, 43, 729  
 Zhang, Y., & Cui, X. Q. 2005, ChJAA (Chin. J. Astron. Astrophys.), 5, 302  
 Zhang, Y. 2005, PhD dissertation of Graduate School of Chinese Academy of Science  
 Zhang, Y. 2006, Proc. SPIE, 6267, 626735  
 Zhang, Y. 2008, Proc. SPIE, 7012, 70123H-70123H-11